HHS Public Access

Author manuscript

Clin Anat. Author manuscript; available in PMC 2019 November 01.

Published in final edited form as:

Clin Anat. 2018 November ; 31(8): 1177–1183. doi:10.1002/ca.23262.

Three-dimensional Femoral Head Coverage in the Standing Position Represents that Measured In-vivo During Gait

Keisuke Uemura, MD, PhD[1], **Penny R. Atkins, BS**[1,2], **Steve A. Maas, PhD**[2,3,4], **Christopher L. Peters, MD**[1,2], and **Andrew E. Anderson, PhD**[1,2,3,5,*]

[1]Department of Orthopaedics, Harold K. Dunn Orthopaedic Research Laboratory, University of Utah, 590 Wakara Way, Salt Lake City, UT, 84108, USA

[2] Department of Bioengineering, University of Utah, James LeVoy Sorenson Molecular Biotechnology Building, 36 S. Wasatch Drive, Rm. 3100, Salt Lake City, UT 84112, USA

[3] Scientific Computing and Imaging Institute, University of Utah, Warnock Engineering Building, 72 S Central Campus Drive, Room 3750, Salt Lake City, UT 84112, USA

[4] Musculoskeletal Research Laboratories, University of Utah, Warnock Engineering Building, 72 S Central Campus Drive, Room 3750, Salt Lake City, UT 84112, USA

[5] Department of Physical Therapy, University of Utah, Dumke Health Professions Building, 520 Wakara Way, Suite 240 Salt Lake City, UT 84108, USA

Abstract

Introduction—Individuals with over- or under-covered hips may develop hip osteoarthritis. Femoral head coverage is typically evaluated using radiographs, and/or computed tomography (CT) or magnetic resonance images obtained supine. Yet, these static assessments of coverage may not provide accurate information regarding the dynamic, three-dimensional (3-D) relationship between the femoral head and acetabulum. The objectives of this study were to: 1) quantify total and regional 3-D femoral head coverage in a standing position and during gait, and 2) quantify the relationship between 3-D femoral head coverage in standing to that measured during gait.

Materials and Methods—The kinematic position of the hip during standing and gait was measured in-vivo for eleven asymptomatic morphologically normal subjects using dual fluoroscopy and model-based tracking of 3-D CT models. Percent coverage in the standing position and during gait was measured overall and on a regional basis (anterior, superior, posterior, inferior). Coverage in standing was correlated with that measured during gait.

Results—For total coverage, very little change in coverage occurred during gait (range: 35.0 – 36.7%; mean: 36.2%). Coverage at each time point of gait strongly correlated with coverage during standing (r = 0.929 – 0.989). The regions thought to play an important role in weight

[*]**Corresponding Author:** Andrew E. Anderson, Ph.D., University of Utah, Department of Orthopaedics, Harold K. Dunn Orthopaedic Research Laboratory, 590 Wakara Way, Salt Lake City, UT 84108, Phone: 801-587-5208, Fax: 801-587-5211, andrew.anderson@hsc.edu.

CONFLICT OF INTEREST STATEMENT

The corresponding author and co-authors do not have a conflict of interest, financial or otherwise, that would inappropriately influence or bias the research reported herein.

bearing (i.e. anterior, superior, posterior) were significantly correlated with coverage in standing during the stance phase.

Conclusions—Our results suggest that coverage measured in a standing position is a good surrogate for coverage measured during gait.

Keywords

hip; morphometrics; femoral head coverage; femur; pelvis; dual fluoroscopy; dynamic; gait analysis

Keywords

Osteoarthritis; Hip Joint; Hip Prosthesis; Hip Dysplasia; Femur Head; Imaging; Three-dimensional; 3-D Imaging; Imaging; 3-D; Computer-Assisted Three-Dimensional Imaging; Gait

INTRODUCTION

Individuals with over- or under-covered hips are at risk of developing hip osteoarthritis (OA) (Beck et al., 2005; Conrozier et al., 1998; Giori and Trousdale, 2003; Gosvig et al., 2010; Kim et al., 2006; Novais et al., 2017; Reijman et al., 2005; Tonnis and Heinecke, 1999). Hip preservation surgery may slow or halt the progression of OA in these patients by changing the anatomic relationship between the femoral head and acetabulum (Kaneuji et al., 2015; Steppacher et al., 2008). In particular, pelvic osteotomies aim to improve cartilage contact mechanics by increasing lateral femoral head coverage in patients with developmental dysplasia of the hip and posterolateral coverage in patients with acetabular retroversion. Osteochondroplasty, which is most often performed arthroscopically, aims to eliminate impingement caused by an overly-prominent acetabular rim in patients with pincer femoroacetabular impingement syndrome and acetabular protrusio.

The success of surgeries to treat structural hip deformities relies, in part, on a thorough pre-operative understanding of femoral head coverage. Most often, two-dimensional (2-D) radiographic measurements of the lateral center-edge angle (LCEA) (Clohisy et al., 2008; Novais et al., 2017; Wiberg, 1953), extrusion index (Murphy et al., 1995), and Tönnis angle (Tonnis and Heinecke, 1999) from an anteroposterior film are used to evaluate femoral head coverage. However, there are several limitations associated with these radiographic measurements. For example, 2-D radiographic measurements are influenced by patient positioning and imaging technique (Kosuge et al., 2014), which may give rise to high inter- and intra-observer error (Kapron et al., 2011). Importantly, each 2-D radiographic measurement provides a single angular measurement of the anatomy, which may not accurately represent the extent of complex, three-dimensional (3-D) deformities known to alter femoral head coverage (Hansen et al., 2012).

Previously, computed tomography (CT) images have been used to calculate 3-D coverage of the femoral head on an overall (Cheng et al., 2015; Dandachli et al., 2008; Miyasaka et al., 2014; Suzuki et al., 2017; van Bosse et al., 2015) and regional basis (Hansen et al., 2012; Larson et al., 2015). A major limitation of these prior studies is that 3-D coverage was based

on reconstructions of volumetric images acquired in the supine position. Previous 2-D radiographic studies found a difference in coverage among supine and standing positions (Henebry and Gaskill, 2013; Pullen et al., 2014; Wylie et al., 2017). Thus, it follows that femoral head coverage could change during gait, but these measurements are not available. As gait is a common daily activity that results in increased stress at the covered region, understanding how coverage changes during gait could influence how structural hip deformities are diagnosed and treated. For example, if it was shown that lateral coverage decreases during gait, then surgeons may wish to reorient the acetabular socket more laterally than they would if they had based the pre-operative plan on only an assessment of coverage during standing.

The objectives of this study were to: 1) quantify total and regional 3-D femoral head coverage in a standing position and during gait, and 2) quantify the relationship between 3-D femoral head coverage measurements in standing to that measured during gait. Our analysis was focused on quantifying coverage in asymptomatic, morphologically-normal, control hips to establish the baseline understanding necessary to study pathologic hips in the future. We hypothesized that: 1) 3-D femoral head coverage measured in the standing position would differ significantly compared to that during the gait cycle, and 2) 3-D measurements of coverage in the standing position would be significantly correlated with 3-D coverage measured dynamically.

MATERIALS ANS METHODS

Subjects

Eighteen pain-free control subjects without a history of injury or surgery to either lower limb signed informed consent to be considered for participation in this Institutional Review Board approved study. These eighteen subjects were screened using an anteroposterior film to exclude individuals with morphological abnormalities, including acetabular dysplasia, femoroacetabular impingement, acetabular retroversion, or Perthes disease. Seven subjects were excluded based on these criteria, leaving eleven subjects (six male). The mean ± standard deviation LCEA, extrusion index, and Tönnis angle for the eleven subjects was 32.8 ± 5.0°, 11.8 ± 4.6, and 3.6 ± 3.7°, respectively. The mean ± standard deviation age, height, and body mass index was 23 ± 2 years, 173 ± 10 cm, and 21 ± 2 kg/m^2, respectively.

CT Scans and Dual Fluoroscopy (DF) Data Collection

The eleven subjects enrolled in this study were previously analyzed using a combined experimental and computational protocol that involved motion capture, CT scan, DF, and model-based markerless tracking (MBT) to calculate in-vivo hip kinematics (Atkins et al., 2017; Fiorentino et al., 2016a; Fiorentino et al., 2017; Fiorentino et al., 2016b; Uemura et al., 2018). Briefly, subjects walked on an instrumented treadmill (Bertec, Columbus, OH, USA) at their self-selected walking speed. Simultaneously, high-speed DF images were acquired at 100 Hz of the pelvis and proximal femur of a randomly-selected hip. DF images were also captured during a static position (i.e. standing position) while subjects stood upright with their feet hip-width apart and pointed forward.

Subjects underwent a CT arthrogram of the hip that was imaged with DF using a 128-slice scanner (SOMATOM Definition, Siemens Healthineers, Erlangen, Germany) with a field of view (300 – 400 mm) that included the entire pelvis, proximal femur, and femoral condyles. The proximal femur and pelvis were scanned with 1 mm slices at 120 kVp and 200 – 400 mAs, and the femoral condyles were scanned at 3 mm slices with 120 kVP and 150 mAs. Caredose™ was used for all scans to modulate tube current. Surface models of the pelvis and the femur were generated by semi-automatic segmentation of the CT images using Amira (v.6.0.1, Visage Imaging, San Diego, CA, USA) (Figure 1A). Finally, MBT used the 3-D bone reconstructions and DF images to calculate the in-vivo position of the pelvis and femur for the standing position and during the entire gait cycle as described previously (Kapron et al., 2014). Two trials of treadmill walking were collected, but the trial with the highest quality fluoroscopy images was chosen for MBT. Of note, we previously validated MBT of the hip to errors less than 0.5 mm and 0.6° (Kapron et al., 2014).

Analysis of Total and Regional Femoral Head Coverage

Analysis of total and regional femoral head coverage was performed using the spatial position of the 3-D reconstructions of the pelvis and femur at each time point in the gait cycle as calculated from the DF images by MBT. Coverage was defined as the area where the lunate surface of the acetabulum covered the femoral head (Collin et al., 2017; Hansen et al., 2012). Triangular elements representing the lunate surface of acetabulum (Figure 1B) and the femoral head (Figure 1C) were extracted from surface models in PostView (Maas et al., 2012) (v.2.0, University of Utah, Salt Lake City, UT, USA) using principle curvature as described previously (Kapron et al., 2014). Briefly, the elements and nodes of the femoral head were automatically selected using 1^{st} principle curvature. Fovea capitis was also excluded using 1^{st} principle curvature. The elements and nodes of the lunate surface were semi-automatically selected from the pelvis model based on 2^{nd} principle curvature values. 2^{nd} principle curvature provided the exclusion of the acetabular fossa, but also excluded the acetabular rim. As such, the lunate surface was expanded manually to include the acetabular rim to ensure the entire bony acetabulum was considered when analyzing coverage.

Using MATLAB (v. 7.10, The MathWorks, Natick, MA, USA), the surface model of the femoral head was divided into four anatomic regions (i.e. anterior, superior, posterior, and inferior) to enable regional coverage calculations and comparisons. Herein, the femoral head coordinate system was defined based on landmarks of the medial and lateral epicondyles, femoral head center, and femoral neck axis. The transverse axis of the femur (Figure 2A) was defined as the long axis of a best-fit cylinder to the surface nodes representing the femoral neck (i.e. neck axis)(Casciaro et al., 2010; Uemura et al., 2018). The superior-inferior axis (Figure 2B) was defined as the axis between the mid-point of the medial and lateral femoral condyles (Wu et al., 2002) and the center of the femoral head, as defined using a sphere-fit (Harris et al., 2013). Using this coordinate system, the nodes of the femoral head were sorted into quadrants about the transverse axis (Figure 2C) (Harris et al., 2014; Wylie et al., 2017).

The Coverage Tool in PostView was used to calculate femoral head coverage. Herein, the surface elements of the femoral head were considered in the calculation of coverage if they

were intersected by the normal projection of any element of the lunate surface. The kinematic data from MBT was applied to the surface models of the lunate surface and femoral head using the Kinemat Tool in PostView. Coverage was assessed for each time point during the gait cycle, and results were exported to MATLAB. First, areal coverage, measured in units of mm^2, was defined by calculating the area of the elements at the femoral head surface that were covered; this calculation was repeated on a regional basis according to the boundaries for each quadrant. Second, recognizing that the size of the femoral head may vary across subjects, areal coverage was converted into a percent coverage by dividing the covered area by the total area overall and with respect to each quadrant. Both areal coverage and percent coverage were calculated at each time point of the gait cycle.

Upon confirming a normal distribution using a Kolmogorov-Smirnov test, percent coverage was expressed as mean ± standard deviation. Comparisons among the regions were made with one-way analysis of variance (ANOVA). Multiple comparisons were corrected by using the Hochberg procedure. Coverage measured in the standing position was compared to the mean coverage measured during gait using a paired Student's t-test. Next, coverage measured in standing for each subject was correlated to that subject's mean coverage during gait using Pearson's correlation. Additionally, for each time point of the gait cycle, coverage during standing was correlated to coverage measured at each time point. In this way, each time point during gait had a corresponding correlation coefficient that was plotted to show whether there were stronger correlations during specific points of the gait cycle. Finally, the intra-class correlation coefficient (ICC) was used to determine the level of agreement in percent coverage calculations by two of the authors (KU, PRA), which was deemed necessary, as there was some manual selection involved (e.g. acetabular rim) when choosing triangular elements to be used for the calculation of coverage. In this case, the ICC assessed agreement in percent coverage in the standing position. For all statistics, $p < 0.05$ was considered to represent significant differences. Correlation coefficients > 0.8 were considered to represent very strong correlations, and ICC values > 0.8 were considered to represent very strong reliability (Landis and Koch, 1977; Uemura et al., 2018). All statistical analyses were performed using SPSS statistical software (v.22, IBM, Armonk, NY, USA).

RESULTS

Unless otherwise noted, all data were presented as mean ± standard deviation. In the standing position, the total coverage of the femoral head was 36.2 ± 2.9% (Table 1). Percent coverage for the anterior, superior, posterior, and inferior regions was 24.4 ± 2.2%, 53.1 ± 6.2%, 51.4 ± 6.0%, and 10.6 ± 3.7%, respectively. There were significant differences in percent coverage between each of the four regions ($p < 0.001$) except between the posterior and superior regions ($p = 0.955$).

During gait, the mean total coverage of the femoral head was 36.2 ± 3.0% when averaged across subjects. The mean percent coverage for the anterior, superior, posterior, and inferior regions was 29.7 ± 3.7%, 51.2 ± 7.1%, 48.8 ± 5.6%, and 9.5 ± 3.0%, respectively (Table 1). Total percent coverage did not vary substantially during gait, ranging from 35.0 – 36.7% (Figure 3). The range in percent coverage for the anterior, superior, posterior, and inferior regions was 16.2 – 39.4%, 48.4 – 56.6%, 41.5 – 55.9%, and 7.4 – 13.6%, respectively

(Figure 3). When analyzing mean data, the total coverage at 30% and 57% of the gait cycle matched that measured during standing (Figure 3, marked as short vertical lines). For each of the regions, the percent coverage was equal to that of the standing position at 31% and 62% of the gait cycle for the anterior region, 52% and 72% for the superior region, 23% and 60% for the posterior region, and 29% and 59% for the inferior region (Figure 3).

On a regional basis, coverage in the standing position was significantly larger than the mean coverage during gait for the posterior and the superior regions and significantly smaller for the anterior region ($p = 0.006$, 0.015, and $p < 0.001$, respectively) (Table 1). However, percent coverage between the standing position and gait only varied by 1.1 – 5.3% (absolute difference in percent coverage, not a percent change).

Mean coverage during gait was significantly correlated to coverage during standing for all regions (Table 1). Correlations between total coverage during gait with coverage during standing were very high and significant for the entire gait cycle ($r = 0.929 – 0.989$) (Figure 4, limit of significant r values shown as a horizontal dashed line at ~0.6). When analyzed regionally, correlations were significant for most of gait cycle (Figure 4).

For the inter-observer analysis, the ICCs of percent total coverage and for all four regions were between 0.823 and 0.999, indicating strong reliability(Landis and Koch, 1977). When considering total and regional coverage together, the mean absolute difference in percent coverage between the observers was 0.2% - 1.1%.

DISCUSSION

Structural hip diseases that present with abnormal femoral head coverage may lead to OA. Hip preservation surgery aims to improve, or in some instances reduce, femoral head coverage so as to normalize hip contact mechanics. Thus, pre-operative measurements of femoral head coverage are deemed important for surgical planning. Femoral head coverage is typically measured from a standing or supine plain film radiograph, and/or from CT or magnetic resonance (MR) images, but these measurements may not be representative of coverage during gait. Therefore, we sought to quantify 3-D femoral head coverage in a standing position as well as during gait. We found little variation in total femoral head coverage during the gait cycle. While we found significant differences on a regional basis when comparing coverage during standing with that during gait, the magnitude of these differences was quite small, and likely not clinically-relevant. We also evaluated the relationship of femoral head coverage during gait with that measured for standing, and found significant correlations for all regions over most of the gait cycle. Thus, collectively, our results suggest that 3-D coverage measured in a standing position is a good surrogate for coverage measured during gait. However, it is important to note that this conclusion is based on an analysis of asymptomatic, morphologically-normal subjects, and could change if patients with hip pathoanatomy were analyzed.

In this study, the mean total percent coverage observed in the standing position was 36.2%, which is smaller than previous studies of normal subjects that reported percent coverage between 40 – 73% (Cheng et al., 2015; Dandachli et al., 2008; Hansen et al., 2012; Larson et

al., 2015; Miyasaka et al., 2014). However, our results are not directly comparable since we defined coverage differently. In particular, a few studies used only the proximal hemisphere of the femoral head to define coverage, which would lead to higher values than our study since we included the entire femoral head (Cheng et al., 2015; Dandachli et al., 2008; Miyasaka et al., 2014). We chose to include the entire femoral head because the distal hemisphere could contact the acetabulum during hip flexion-extension or abduction-adduction. Other reports included the fovea capitis and the acetabular fossa when calculating coverage (Hansen et al., 2012; Larson et al., 2015), which could give rise to higher percent coverage values than those measured in our study. We chose not to include the fovea capitis and acetabular fossa, as it would be highly unlikely that these recessed regions would ever be in contact. Consistent with previous studies of control subjects, we found coverage to be greater in the posterior region than in the anterior region (Hansen et al., 2012; Larson et al., 2015). We also found coverage in the inferior region to be the smallest among the four regions, which was likely due to exclusion of the acetabular fossa.

Our first hypothesis that femoral head coverage would change during gait was confirmed for the anterior, posterior and superior regions, but not for total coverage or for the inferior region. It is important to recognize that, although statistically significant, the differences may not be clinically-meaningful, as they were quite small (difference of 1.9 – 5.3%, calculated as 23 – 67 mm^2). We previously showed that hip translation during gait in these subjects was only 0.6 mm (Fiorentino et al., 2016a). Such small translations are unlikely to move the femoral head center enough to have a major impact on coverage, especially if the hip is spherical in shape. However, we posit that coverage may change more for patients with structural hip disease. In particular, many patients with acetabular dysplasia have irregularly-shaped femoral heads that may subluxate during articulation, which could reduce or increase coverage depending on the direction the hip translates. Similarly, coverage may change more during dynamic motion for patients with cam-type FAI since the hip may translate laterally as the aspherical femoral head attempts to articulate with a spherically-shaped acetabulum.

Our second hypothesis that coverage in the standing position would correlate with coverage measured during gait was confirmed for total coverage when correlated with coverage during standing over the entire gait cycle, and for most of the gait cycle when correlations were performed on a regional basis. The correlation observed in the inferior region over the gait cycle tended to be lower than other regions. This finding may be due to structural variations in the shape of the acetabular fossa across subjects, as the inferior region faces the acetabular fossa during most of the gait cycle. However, it is important to note that the regions which play an important role in weight bearing (i.e. anterior, superior, and posterior) were significantly correlated during the stance phase, and that the total coverage was very strongly correlated.

The advantage of using CT, DF, and MBT for this study was that in-vivo 3-D femoral head coverage was measured in both standing and during gait. However, there were some limitations. First, the contact area between the femoral head and the acetabulum may vary with the inclusion of cartilage and labrum anatomies. However, our primary purpose was to quantify femoral head coverage based on the bony anatomy, as it is the bony structures of

the acetabulum and femur that are examined in a clinical setting to diagnose and treat structural hip disease. Second, this study only included asymptomatic subjects as our goal was to gain a baseline understanding of coverage for future comparisons to patients. As explained above, it is possible that patients with structural hip disease have more or less pronounced differences in coverage between standing and during gait. Third, we only analyzed coverage during standing and gait; activities that require larger range of motion at the hip may demonstrate larger changes in coverage from the reference standing position. Fourth, we did not measure coverage in the supine position because we had used traction during the CT scan, which caused the femur to be displaced inferiorly, and induced changes in pelvic obliquity and tilt as a result. As such, we felt that calculating coverage in the supine position as based on the CT images would bias the results because subjects had varying amounts of inferior displacement and pelvis tilt and obliquity as a result of traction. Finally, subjects were exposed to ionizing radiation. The estimated maximum amount received was 10.72mSv, which amounts to 21% of the annual exposure limit for a radiation worker (Fiorentino et al., 2017).

In conclusion, our findings indicate that 3-D head coverage analysis based on a standing position can be applied cautiously to express the coverage during gait. Future work will expand the current study to include patients with structural hip deformities. Nevertheless, the results reported herein for normal controls provide valuable baseline data which can be used in the evaluation of pathological patients in the future.

ACKNOWLEDGEMENTS

This work was supported by grants from the National Institutes of Health (NIH) (R21 AR063844, S10 RR026565, F32 AR067075), the LS-Peery Discovery Program in Musculoskeletal Restoration, the LS Peery Discovery Program in Musculoskeletal Restoration, the Nakatomi Foundation, and the Nakatani Foundation for Advancement of Measuring Technologies in Biomedical Engineering. The research content herein is solely the responsibility of the authors and does not necessarily represent the official views of the NIH or other foundations

REFERENCES

Atkins PR, Fiorentino NM, Aoki SK, Peters CL, Maak TG, Anderson AE. 2017 In Vivo Measurements of the Ischiofemoral Space in Recreationally Active Participants During Dynamic Activities: A High-Speed Dual Fluoroscopy Study. Am J Sports Med 45:2901–2910. [PubMed: 28682639]

Beck M, Kalhor M, Leunig M, Ganz R. 2005 Hip morphology influences the pattern of damage to the acetabular cartilage: femoroacetabular impingement as a cause of early osteoarthritis of the hip. J Bone Joint Surg Br 87:1012–1018. [PubMed: 15972923]

Casciaro ME, Ritacco LE, Milano F, Risk M, Craiem D. 2010 Angle estimation of human femora in a three-dimensional virtual environment. Conf Proc IEEE Eng Med Biol Soc 2010:3946–3949.

Cheng H, Liu L, Yu W, Zhang H, Luo D, Zheng G. 2015 Comparison of 2.5D and 3D Quantification of Femoral Head Coverage in Normal Control Subjects and Patients with Hip Dysplasia. PLoS One 10:e0143498. [PubMed: 26599869]

Clohisy JC, Carlisle JC, Beaule PE, Kim YJ, Trousdale RT, Sierra RJ, Leunig M, Schoenecker PL, Millis MB. 2008 A systematic approach to the plain radiographic evaluation of the young adult hip. J Bone Joint Surg Am 90 Suppl 4:47–66.

Collin PG, D'Antoni AV, Loukas M, Oskouian RJ, Tubbs RS. 2017 Hip fractures in the elderly-: A Clinical Anatomy Review. Clin Anat 30:89–97. [PubMed: 27576301]

Conrozier T, Jousseaume CA, Mathieu P, Tron AM, Caton J, Bejui J, Vignon E. 1998 Quantitative measurement of joint space narrowing progression in hip osteoarthritis: a longitudinal retrospective study of patients treated by total hip arthroplasty. Br J Rheumatol 37:961–968. [PubMed: 9783760]

Dandachli W, Kannan V, Richards R, Shah Z, Hall-Craggs M, Witt J. 2008 Analysis of cover of the femoral head in normal and dysplastic hips: new CT-based technique. J Bone Joint Surg Br 90:1428–1434. [PubMed: 18978260]

Fiorentino NM, Atkins PR, Kutschke MJ, Foreman KB, Anderson AE. 2016a In-vivo quantification of dynamic hip joint center errors and soft tissue artifact. Gait Posture 50:246–251. [PubMed: 27693944]

Fiorentino NM, Atkins PR, Kutschke MJ, Goebel JM, Foreman KB, Anderson AE. 2017 Soft tissue artifact causes significant errors in the calculation of joint angles and range of motion at the hip. Gait Posture 55:184–190. [PubMed: 28475981]

Fiorentino NM, Kutschke MJ, Atkins PR, Foreman KB, Kapron AL, Anderson AE. 2016b Accuracy of Functional and Predictive Methods to Calculate the Hip Joint Center in Young Non-pathologic Asymptomatic Adults with Dual Fluoroscopy as a Reference Standard. Ann Biomed Eng 44:2168–2180. [PubMed: 26645080]

Giori NJ, Trousdale RT. 2003 Acetabular retroversion is associated with osteoarthritis of the hip. Clin Orthop Relat Res:263–269. [PubMed: 14646725]

Gosvig KK, Jacobsen S, Sonne-Holm S, Palm H, Troelsen A. 2010 Prevalence of malformations of the hip joint and their relationship to sex, groin pain, and risk of osteoarthritis: a population-based survey. J Bone Joint Surg Am 92:1162–1169. [PubMed: 20439662]

Hansen BJ, Harris MD, Anderson LA, Peters CL, Weiss JA, Anderson AE. 2012 Correlation between radiographic measures of acetabular morphology with 3D femoral head coverage in patients with acetabular retroversion. Acta Orthop 83:233–239. [PubMed: 22553905]

Harris MD, Kapron AL, Peters CL, Anderson AE. 2014 Correlations between the alpha angle and femoral head asphericity: Implications and recommendations for the diagnosis of cam femoroacetabular impingement. Eur J Radiol 83:788–796. [PubMed: 24613175]

Harris MD, Reese SP, Peters CL, Weiss JA, Anderson AE. 2013 Three-dimensional quantification of femoral head shape in controls and patients with cam-type femoroacetabular impingement. Ann Biomed Eng 41:1162–1171. [PubMed: 23413103]

Henebry A, Gaskill T. 2013 The effect of pelvic tilt on radiographic markers of acetabular coverage. Am J Sports Med 41:2599–2603. [PubMed: 23982398]

Kaneuji A, Sugimori T, Ichiseki T, Fukui K, Takahashi E, Matsumoto T. 2015 Rotational Acetabular Osteotomy for Osteoarthritis with Acetabular Dysplasia: Conversion Rate to Total Hip Arthroplasty within Twenty Years and Osteoarthritis Progression After a Minimum of Twenty Years. J Bone Joint Surg Am 97:726–732. [PubMed: 25948519]

Kapron AL, Anderson AE, Aoki SK, Phillips LG, Petron DJ, Toth R, Peters CL. 2011 Radiographic prevalence of femoroacetabular impingement in collegiate football players: AAOS Exhibit Selection. J Bone Joint Surg Am 93:e111(111–110).

Kapron AL, Aoki SK, Peters CL, Maas SA, Bey MJ, Zauel R, Anderson AE. 2014 Accuracy and feasibility of dual fluoroscopy and model-based tracking to quantify in vivo hip kinematics during clinical exams. J Appl Biomech 30:461–470. [PubMed: 24584728]

Kim WY, Hutchinson CE, Andrew JG, Allen PD. 2006 The relationship between acetabular retroversion and osteoarthritis of the hip. J Bone Joint Surg Br 88:727–729. [PubMed: 16720763]

Kosuge D, Cordier T, Solomon LB, Howie DW. 2014 Dilemmas in imaging for peri-acetabular osteotomy: the influence of patient position and imaging technique on the radiological features of hip dysplasia. Bone Joint J 96-b:1155–1160. [PubMed: 25183583]

Landis JR, Koch GG. 1977 The measurement of observer agreement for categorical data. Biometrics 33:159–174. [PubMed: 843571]

Larson CM, Moreau-Gaudry A, Kelly BT, Byrd JW, Tonetti J, Lavallee S, Chabanas L, Barrier G, Bedi A. 2015 Are normal hips being labeled as pathologic? A CT-based method for defining normal acetabular coverage. Clin Orthop Relat Res 473:1247–1254. [PubMed: 25407391]

Maas SA, Ellis BJ, Ateshian GA, Weiss JA. 2012 FEBio: finite elements for biomechanics. J Biomech Eng 134:011005. [PubMed: 22482660]

Miyasaka D, Ito T, Imai N, Suda K, Minato I, Dohmae Y, Endo N. 2014 Three-dimensional Assessment of Femoral Head Coverage in Normal and Dysplastic Hips: A Novel Method. Acta Med Okayama 68:277–284. [PubMed: 25338484]

Murphy SB, Ganz R, Muller ME. 1995 The prognosis in untreated dysplasia of the hip. A study of radiographic factors that predict the outcome. J Bone Joint Surg Am 77:985–989. [PubMed: 7608241]

Novais EN, Duncan S, Nepple J, Pashos G, Schoenecker PL, Clohisy JC. 2017 Do Radiographic Parameters of Dysplasia Improve to Normal Ranges After Bernese Periacetabular Osteotomy? Clin Orthop Relat Res 475:1120–1127. [PubMed: 27646418]

Pullen WM, Henebry A, Gaskill T. 2014 Variability of acetabular coverage between supine and weightbearing pelvic radiographs. Am J Sports Med 42:2643–2648. [PubMed: 25214530]

Reijman M, Hazes JM, Pols HA, Koes BW, Bierma-Zeinstra SM. 2005 Acetabular dysplasia predicts incident osteoarthritis of the hip: the Rotterdam study. Arthritis Rheum 52:787–793. [PubMed: 15751071]

Steppacher SD, Tannast M, Ganz R, Siebenrock KA. 2008 Mean 20-year followup of Bernese periacetabular osteotomy. Clin Orthop Relat Res 466:1633–1644. [PubMed: 18449617]

Suzuki D, Nagoya S, Takashima H, Tateda K, Yamashita T. 2017 Three-dimensional orientation of the acetabulum. Clin Anat 30:753–760. [PubMed: 28631289]

Tonnis D, Heinecke A. 1999 Acetabular and femoral anteversion: relationship with osteoarthritis of the hip. J Bone Joint Surg Am 81:1747–1770. [PubMed: 10608388]

Uemura K, Atkins PR, Fiorentino NM, Anderson AE. 2018 Hip rotation during standing and dynamic activities and the compensatory effect of femoral anteversion: An in-vivo analysis of asymptomatic young adults using three-dimensional computed tomography models and dual fluoroscopy. Gait Posture 61:276–281. [PubMed: 29413797]

van Bosse H, Wedge JH, Babyn P. 2015 How are dysplastic hips different? A three-dimensional CT study. Clin Orthop Relat Res 473:1712–1723. [PubMed: 25524428]

Wiberg G 1953 Shelf operation in congenital dysplasia of the acetabulum and in subluxation and dislocation of the hip. J Bone Joint Surg Am 35-a:65–80. [PubMed: 13022708]

Wu G, Siegler S, Allard P, Kirtley C, Leardini A, Rosenbaum D, Whittle M, D'Lima DD, Cristofolini L, Witte H, Schmid O, Stokes I. 2002 ISB recommendation on definitions of joint coordinate system of various joints for the reporting of human joint motion--part I: ankle, hip, and spine. International Society of Biomechanics. J Biomech 35:543–548. [PubMed: 11934426]

Wylie JD, Kapron AL, Peters CL, Aoki SK, Maak TG. 2017 Relationship Between the Lateral Center-Edge Angle and 3-Dimensional Acetabular Coverage. Orthop J Sports Med 5:2325967117700589. [PubMed: 28451616]

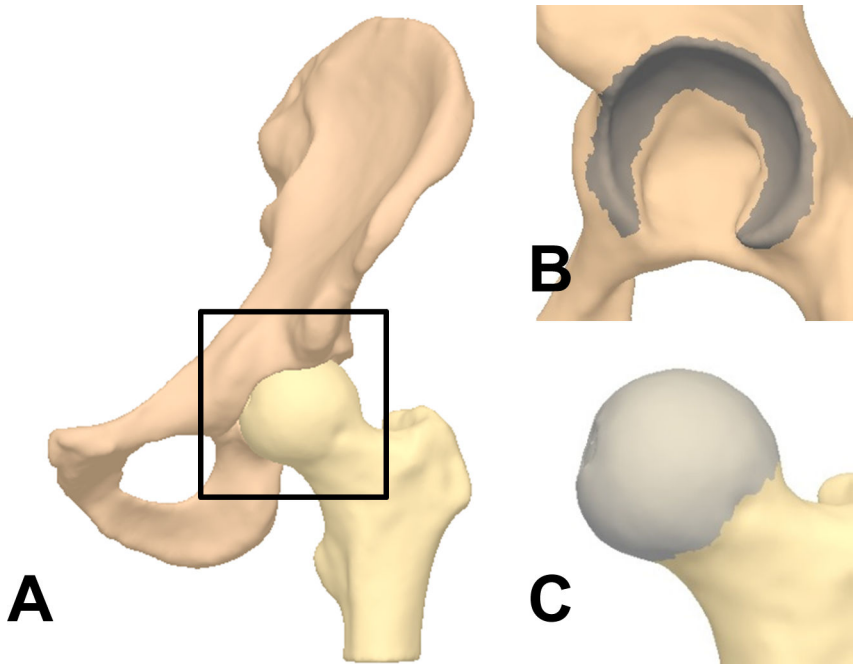

Figure 1.

Three-dimensional surface models of the lunate surface and the femoral head used to calculate coverage. (A) Surface models of the pelvis (superior) and the femur (inferior) were generated from computed tomography images. (B) The lunate surface (dark gray) was semi-automatically selected from the pelvis surface model using 2nd principle curvature and manual selection. (C) The femoral head (light gray) was automatically selected from the femur model using 1st principle curvature.

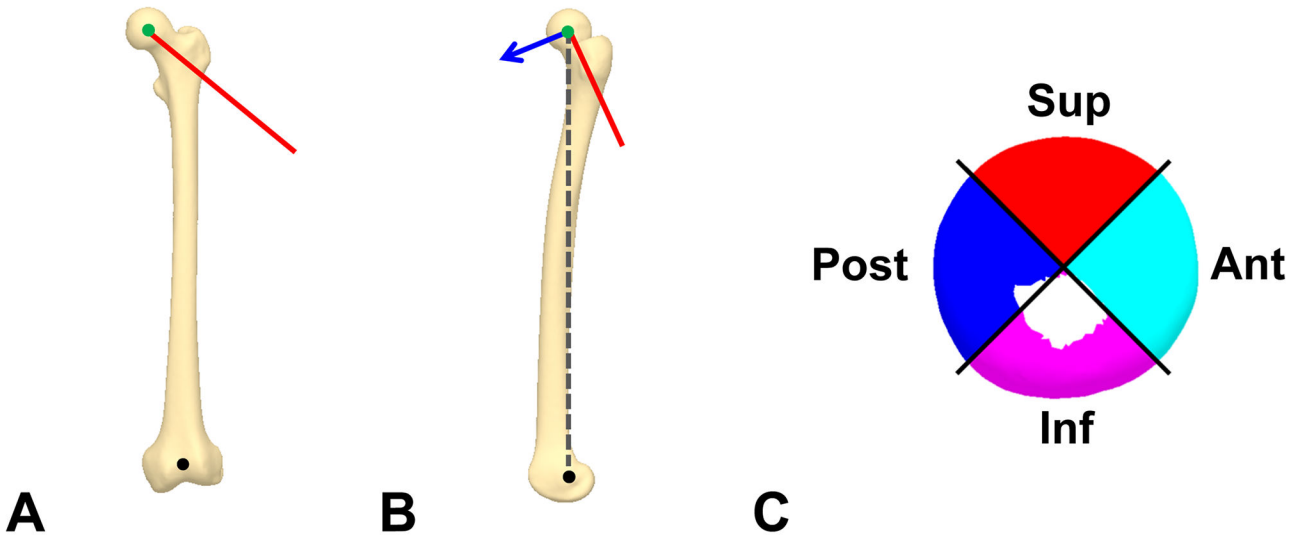

Figure 2.

A femoral coordinate system was defined and used to classify the femoral head into four regions. (A) The femoral head center (green circle), knee center (black circle), and neck axis (red line) were defined from the surface model of the femur. The neck axis was used to define the central vector separating the four regions. (B) The anterior axis (blue arrow) was set as a vector orthogonal to the neck axis and the vector through the centers of the knee and the femoral head (gray dotted line). (C) Using these axes, the nodes of the femoral head were sorted into four regions around the neck axis in 90° increments. Ant, anterior; sup, superior; post, posterior; inf, inferior.

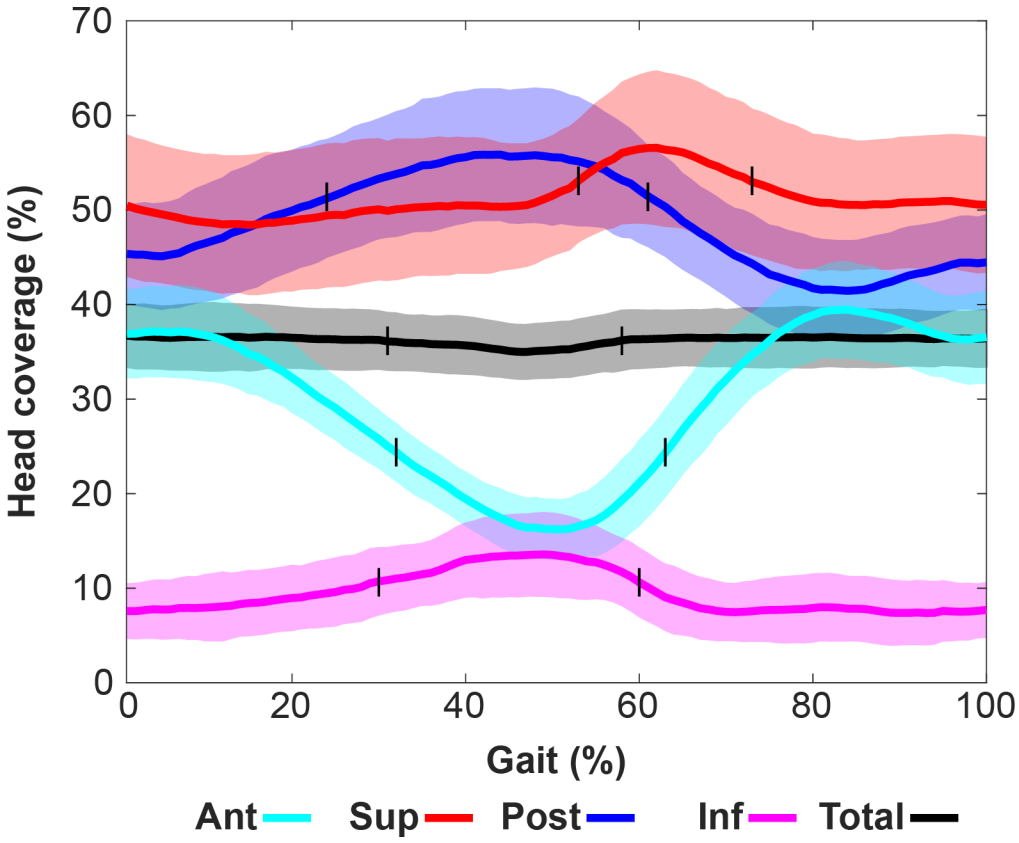

Figure 3.

Mean percent femoral head coverage during gait over the time-normalized gait cycle for the four regions and overall. Percent head coverage presented as mean (solid line) ± standard deviation (shaded area). Short vertical black lines represent the time point when the percent coverage was equivalent to the standing position. Ant, anterior; sup, superior; post, posterior; inf, inferior.

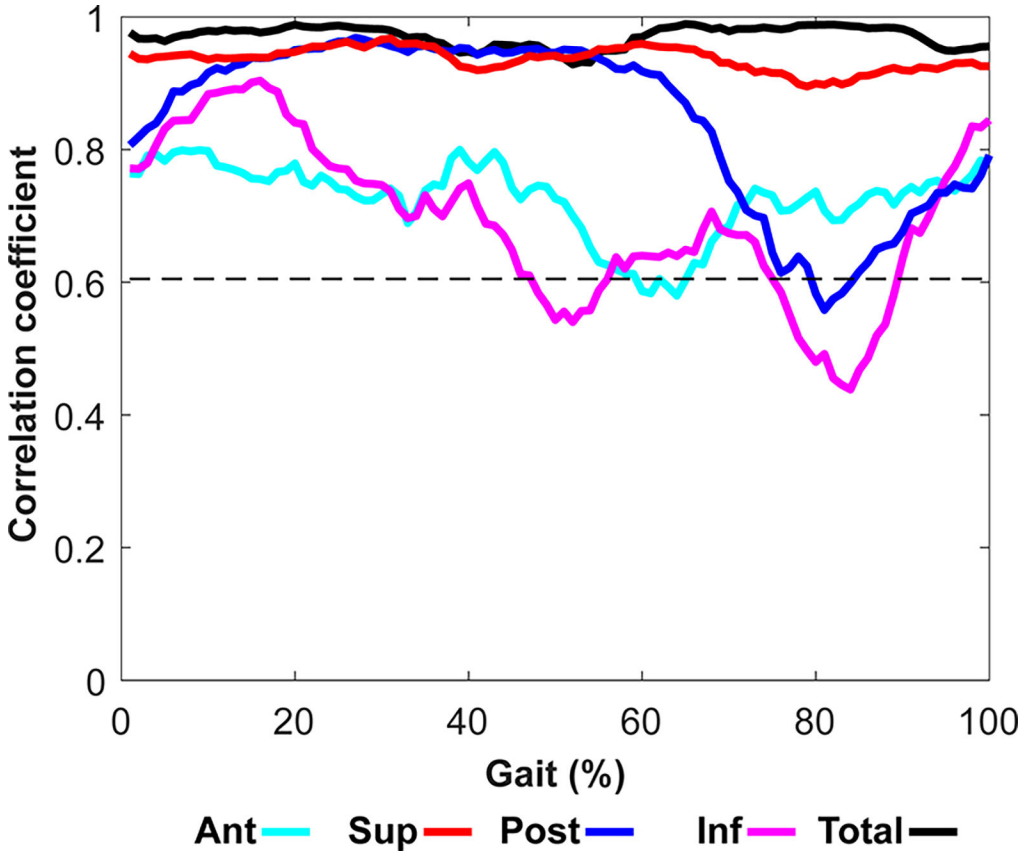

Figure 4.

Correlation between 3-D coverage in the standing position and dynamic 3-D coverage over the time-normalized gait cycle. The black dotted line indicates the minimum significant correlation coefficient (r = 0.605). Ant, anterior; inf, inferior; post, posterior; sup, superior.

TABLE 1.

Area and Percent Coverage of Each Femoral Head Region in the Standing Position and During Gait

Region	Mean area (mm^2) (Percent of the total area)	Mean percent coverage in standing (%)	Mean percent coverage during gait (%)	Difference of mean percent coverage in standing and during gait (%) p-value	Correlation in mean percent coverage between standing and gait
Anterior	1270.2 ± 840.3 (27.4%)	24.4 ± 2.2	29.7 ± 3.7	−5.3 ± 2.3 $p < 0.001$	$r = 0.820$ $p = 0.002$
Inferior	932.0 ± 146.2 (20.1%)	10.6 ± 3.7	9.5 ± 3.0	1.1 ± 2.1 $p = 0.107$	$r = 0.823$ $p = 0.002$
Posterior	1203.1 ± 217.8 (25.9%)	51.4 ± 6.0	48.8 ± 5.6	2.6 ± 2.5 $p = 0.006$	$r = 0.910$ $p < 0.001$
Superior	1232.2 ± 258.9 (26.6%)	53.1 ± 6.2	51.2 ± 7.1	1.9 ± 2.1 $p = 0.015$	$r = 0.961$ $p < 0.001$
Total	4637.5 ± 840.3 (100%)	36.2 ± 2.9	36.2 ± 3.0	−0.1 ± 0.5 $p = 0.705$	$r = 0.989$ $p < 0.001$

Mean area and percent coverage are expressed relative to the area of the femoral head and of each region of the head.